

An Automatic Procedure to Convert ECGs from Graph Paper to Digital Signals

⁽¹⁾ M Paterni, ⁽¹⁾ A Belardinelli, ⁽¹⁾ A Benassi, ⁽¹⁾ C Carpeggiani, ⁽¹⁾ ⁽²⁾ M Demi

⁽¹⁾ CNR – Institute of Clinical Physiology, Pisa, Italy, ⁽²⁾ Esaote S.p.A., Florence, Italy

Abstract

Today most commercial equipment already provides ECG signals in a digital form and allow their registration in a local archive. However, the recovery of past ECGs from graph paper is still needed since ECGs are a valuable source of information regarding the clinical history of a patient and, consequently, it is very useful to have all the ECG recordings of the same patient in the same digital archive for subsequent analyses and comparisons. In this paper we propose a new method to convert ECGs from graph paper to digital signals. First a digital image of the ECG on graph paper is obtained with a flatbed scanner (600 dpi) and then a line detection procedure is used to detect and locate the ECG trace. The first order absolute moment (FOAM) is used as a mathematical operator to highlight the ECG trace with a ridge and the ECG signal is subsequently located at the top of the ridge with a multi-resolution approach.

1. Introduction

The acquisition and the management of ECG data are two very common tasks in every clinical structure. Today commercial equipment mostly provide both a standard output on graph paper and a digital signal which can be stored in a local archive. The management of ECG data in a digital form, however, is not simple since the signals stored in a local archive often cannot be transferred to a different archive because of the different coding systems. Moreover, equipment that does not provide the digital signals as a standard output is still used and in this case, paper is the only means of storing the ECG recordings. Therefore, since the paperless management of ECGs is not yet possible, the recovery of digital signals from past ECGs on graph paper is a common request received from physicians.

The subject of this paper is the development of the software procedures which are needed to recover past ECGs from graph paper. The first order absolute moment (FOAM) is used as a mathematical operator to highlight the ECG trace. A study of this operator [1] shows how the FOAM highlights, with a single ridge, both the edges

and the lines which are present in an image. Given a predefined width w , the FOAM provides a ridge along every line the thickness of which is less than w , and the height of such a ridge increases both when the contrast of the line increases and when the thickness of the line increases from 0 to w pixels. Therefore, if the right configuration of the FOAM is chosen on the basis of the trace thickness, the relative ridge is higher than those produced by the lines of the graph paper, since the ECG trace is commonly both more contrasted and thicker than the lines of the background grid. Consequently, the ridge which corresponds to the ECG trace is easily separated from the other ridges with a simple thresholding operation. A procedure which searches for local maxima is then used to locate the details of the ECG trace at the top of the relative ridge with a multi-resolution approach. Moreover, the orientation of the lines of the background grid is computed and the recovered ECG signal is realigned accordingly. The original paper support can be also subjected to enlargement or reduction before the acquisition phase. Therefore, the mean distance between every pair of adjacent lines of the background grid is computed and the recovered signal is rescaled in order to compensate a possible magnification.

2. The first order absolute moment

In this section the output of the first absolute central moment is analyzed at ideal pulse functions. Let $f(x,y)$ be the gray level map of an image, and let $g(\tau_x, \tau_y, \sigma)$ be a Gaussian weight function with a unitary integral, the first absolute central moment can be written as follows:

$$e(x,y) = \int_{-\infty}^{\infty} \int_{-\infty}^{\infty} |f(x,y) \otimes g(x,y,\sigma_1) + f(x-\tau_x, y-\tau_y)| g(\tau_x, \tau_y, \sigma_2) d\tau_x d\tau_y \quad (1)$$

where the symbol \otimes is the convolution operator. In [1] we have shown how at gray-level discontinuities the absolute central moment provides a single ridge as well as a classical Gradient of Gaussian (GoG) filter. We have also shown how a configuration with $\sigma_1 < \sigma_2$ should be used to cope with noise correctly. Let us now consider

the following ideal pulse function as a test image:

$$f(x, y) = \begin{cases} 0 & x < -\frac{A}{2} \\ H & -\frac{A}{2} \leq x \leq \frac{A}{2} \\ 0 & x > \frac{A}{2} \end{cases} \quad (2)$$

If eq.(1) is computed at a point p the following equation is obtained

$$e(\varepsilon) = -\frac{|H|}{2} \left\{ \left[\operatorname{erf}\left(\frac{\sqrt{2}(A+2\varepsilon)}{4\sigma_1}\right) + \operatorname{erf}\left(\frac{\sqrt{2}(A-2\varepsilon)}{4\sigma_1}\right) - 1 \right] \right. \\ \left. \left[\operatorname{erf}\left(\frac{\sqrt{2}(A+2\varepsilon)}{4\sigma_3}\right) + \operatorname{erf}\left(\frac{\sqrt{2}(A-2\varepsilon)}{4\sigma_3}\right) - 1 \right] - 1 \right\} \quad (3)$$

where $|\varepsilon|$ is the distance of p from the center line of the pulse function. Eq.(3) provides either a local maximum or a local minimum at the center line of the pulse function. Indeed, the first derivative of eq.(3) when computed with respect to ε at the point $\varepsilon=0$ is equal to zero independently of the values of A , σ_1 and σ_3 . If the second derivative of eq.(3) is computed with respect to ε at the point $\varepsilon=0$ then the following relationship is obtained:

$$\frac{\partial^2 e}{\partial \varepsilon^2} \Big|_{(\varepsilon=0)} = \frac{|H|\sqrt{2}}{2A^2\sqrt{\pi}} \left[\frac{A^3}{\sigma_1^3} e^{-\frac{A^2}{8\sigma_1^2}} \left(2\operatorname{erf}\left(\frac{A\sqrt{2}}{4\sigma_1}\right) - 1 \right) + \right. \\ \left. + \frac{A^3}{\sigma_3^3} e^{-\frac{A^2}{8\sigma_3^2}} \left(2\operatorname{erf}\left(\frac{A\sqrt{2}}{4\sigma_3}\right) - 1 \right) \right] \quad (4)$$

Eq.(3) provides a local maximum at the center line of the pulse function when eq.(4) is less than zero. Let σ_1 , σ_3 and A be greater than zero, it is easy to demonstrate with a few steps that eq.(4) is less than zero when the following relationship is satisfied:

$$A_1^3 e^{\frac{1}{8A_1^2}} \left(2\operatorname{erf}\left(\frac{\sqrt{2}}{4A_1}\right) - 1 \right) + A_3^3 e^{\frac{1}{8A_3^2}} \left(2\operatorname{erf}\left(\frac{\sqrt{2}}{4A_3}\right) - 1 \right) < 0 \quad (5)$$

where $A_1 = \sigma_1/A$ and $A_3 = \sigma_3/A$. Let us take the following function into account:

$$y = x^3 e^{\frac{1}{8x^2}} \left(2\operatorname{erf}\left(\frac{\sqrt{2}}{4x}\right) - 1 \right) \quad (6)$$

The function $y(x)$ in eq.(6) for positive values of x is a monotonic non increasing function which tends quickly to infinite when x tends to zero and tends to minus infinite when x tends to infinite. The function $y(x)$ is less

than zero if x is approximately greater than 0.74. Therefore, if both A_1 and A_3 are greater than 0.74 eq.(5) is surely satisfied. This means that the first absolute central moment provides a local maximum at the center line of a pulse function when both σ_1 and σ_3 are greater than 0.74A where A is the width of the pulse. However, eq.(5) is also satisfied if one of the two values A_1 or A_3 is slightly greater than zero (for example >0.2) and the other one is slightly greater than 0.74 (for example >1). Therefore, since σ_1 must be less than σ_3 to cope with noise correctly, then a configuration with $0.2A < \sigma_1 < \sigma_3$ and $\sigma_3 > A$ should be used to provide a local maximum at a pulse function.

Let us now investigate how the height of the ridge, which is provided by eq.(3) at the pulse function, varies when varying the configuration of the mathematical operator. If eq.(3) is computed when $\varepsilon=0$ the following relationship is obtained:

$$e(0) = -|H| \left[2\operatorname{erf}\left(\frac{A\sqrt{2}}{4\sigma_1}\right) \operatorname{erf}\left(\frac{A\sqrt{2}}{4\sigma_3}\right) - \operatorname{erf}\left(\frac{A\sqrt{2}}{4\sigma_1}\right) - \operatorname{erf}\left(\frac{A\sqrt{2}}{4\sigma_3}\right) \right] \quad (7)$$

Let us compute the first derivative of eq.(7) with respect to σ_1 and σ_3 .

$$\frac{\partial e(0)}{\partial \sigma_1} = \frac{A|H|\sqrt{2}}{\sqrt{\pi}\sigma_1^2} e^{-\frac{A^2}{8\sigma_1^2}} \left(\operatorname{erf}\left(\frac{A\sqrt{2}}{4\sigma_1}\right) - \frac{1}{2} \right) \quad (8)$$

$$\frac{\partial e(0)}{\partial \sigma_3} = \frac{A|H|\sqrt{2}}{\sqrt{\pi}\sigma_3^2} e^{-\frac{A^2}{8\sigma_3^2}} \left(\operatorname{erf}\left(\frac{A\sqrt{2}}{4\sigma_3}\right) - \frac{1}{2} \right) \quad (9)$$

According to eq.(8) the height of the ridge increases when increasing σ_1 only if σ_3 is less than 0.74A. However, a configuration with $\sigma_3 > A$ must be used to cope with noise correctly and, consequently, the height of the ridge always decreases when increasing σ_1 . On the other hand, according to eq.(9), the height of the ridge increases when increasing σ_3 if σ_1 is less than 0.74A.

3. Signal realignment

The correction of the trace orientation is the first problem to deal with since possible errors regarding the alignment of the paper to the borders of the glass of the scanner must be compensated. A region of the image (ROI₁) of 360X240 pixels, where only the background grid is present, is selected either automatically or manually. The ROI₁ is subsequently processed with the FOAM filter in order to highlight each line of the grid with a ridge. A configuration with $\sigma_1=1$ pixel ($0.2A_{MAX} < \sigma_1 < \sigma_3$) and $\sigma_3=5$ pixels ($\sigma_3 > A_{MAX}$) was used in this case for the FOAM operator since the thickness of the grid lines on the acquired images varied between 1

and Δ pixels. Let $p_0 \equiv (x_0, y_0)$ be the upper left corner of the ROI₁ as in Fig.1. By moving from p_0 to the lower left corner of the ROI₁ on the filtered image the procedure analyses the lines passing through every point $p_i \equiv (x_i, y_i)$ which have an angular coefficient included within a reasonable interval of realignment $\pm 8^\circ$. For every point $p_i \equiv (x_i, y_i)$ the procedure searches for the angular coefficient m_i of the line that maximizes the mean gray level of the pixels lying on the line itself. At the end of the procedure a function $R(y_i)$ and the list of the angular coefficients m_i of the lines which provide the maximum mean gray level are obtained. In Fig.1 the behavior of $R(y_i)$ is shown. Every peak of the function $R(y_i)$ is associated to a straight line which overlaps a grid line. Once all the local maxima of the function $R(y_i)$ are localized, the mean value of the relative angular coefficients m_i provides us with an estimate α of the grid orientation. The entire ECG image can be now rotated to an angle $-\alpha$. Moreover, the scale factor of the ECG signal is obtained by computing the mean distance between every pair of adjacent lines of the grid. In particular, the scale factor must be computed when the acquired record is a hard copy since, in this case, the original scale factor could have been modified.

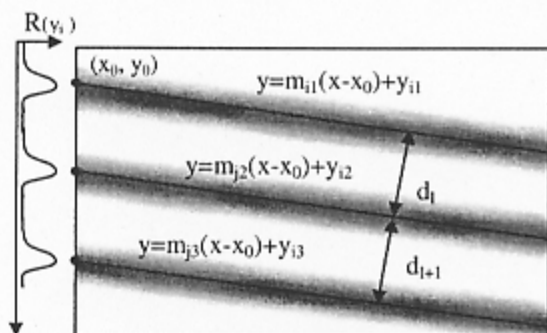


Figure 1. The filtered image and the graph of the function $R(y_i)$ which allow us to detect the grid position and orientation are shown.

4. Background subtraction

A region ROI₂ which includes the ECG trace is provided either automatically or manually and then filtered with the FOAM filter. In this case, the filter configuration must guarantee a high ridge on the trace, a low ridge on the grid lines and must be robust against noise. These requirements demand greater values of σ_1 and σ_2 at this stage of the procedure where the most important problem is the separation of the ECG trace from the background. A configuration with $\sigma_1=3$ pixels and $\sigma_2=12$ pixels was used for the FOAM operator. In this case the FOAM provides a ridge the height of which increases when the thickness of the pulse function

increases from 0 to 6 pixels (the trace thickness). Since the FOAM provides the highest ridge at the thickest pulse function, and since the ECG trace is thicker than the background grid lines, then the ECG trace gives rise to a higher ridge than the grid lines. Therefore, the background can be removed by removing all the pixels of the filtered image whose value is less than a threshold. A threshold $Th(x_i)$ is computed for each column x_i of ROI₂ as $Th(x_i) = \text{MIN}x_i + c(\text{MAX}x_i - \text{MIN}x_i)$ where $\text{MAX}x_i$ is the highest local maximum of $e(x_i, y_i)$ on the column x_i , $\text{MIN}x_i$ is the lowest local maximum of $e(x_i, y_i)$ on the column x_i and c is an arbitrary value. In this work a value of $c=0.6$ was used.

5. Signal localization

With the previous thresholding procedure we expect to completely eliminate almost all the points of the ridges associated to the grid lines and to other sources of errors. We expect also an image $e_{Th}(x_i, y_i)$ where the ridge associated to the ECG trace is still present and does not show many gaps. In other words, we expect an image where the signal is still well defined although random and point-like noise is superimposed. Assuming that, most of the columns of ROI₂ of the image map $e_{Th}(x_i, y_i)$ show a single peak and most of them belong to the ECG trace. Therefore, the localization procedure searches for a single peak in every column of ROI₂. If a single peak is found, that peak is considered a valid point of the ECG trace. If multiple peaks are found then the valid peak is the peak which is closer to the nearest single peak of an adjacent column [2].

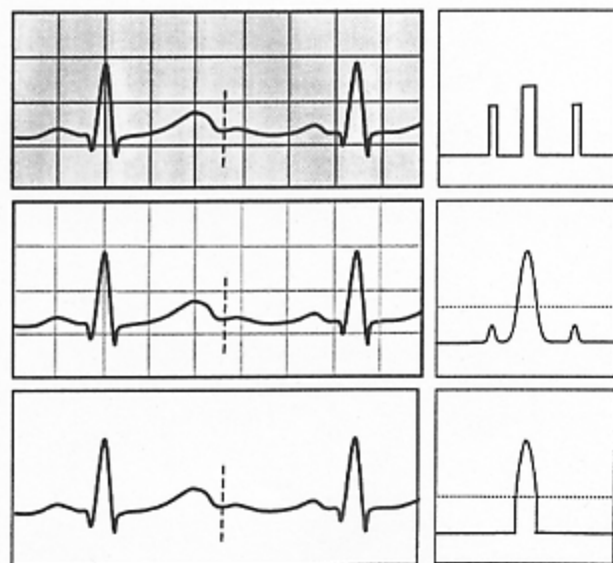


Figure 2. From top to bottom: original image; filtered image which shows a higher ridge on the ECG trace and lower ridges on the grid lines; filtered image after the thresholding process.

All the chosen peaks are subsequently revised and if the distance between a peak p and the two adjacent peaks is greater than a threshold then p is discarded. At the end of this stage all the obtained peaks are interpolated with a polygonal line and a curve which approximates the ECG trace is obtained. Once the above polygonal line is obtained it is used as an approximate starting curve C_1 to locate a more precise curve C_2 at the top of the ridge provided by a new filtering stage with smaller apertures σ_1 and σ_3 . In this case the localization procedure searches for the top of the ridge along the path which is orthogonal to C_1 . In theory C_2 could be used in turn to locate a more precise trace at the top of the ridge which has been provided by a new filtering process and so on until the required precision is obtained.

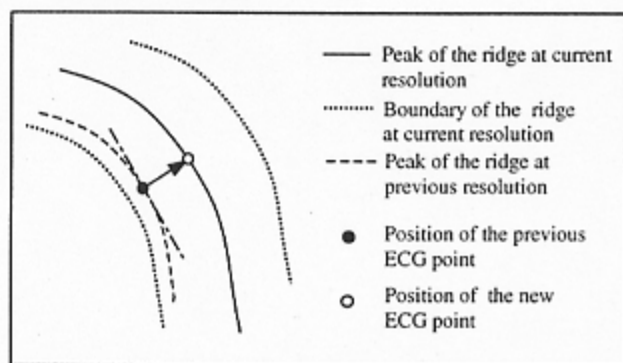


Figure 3. An approximate starting curve can be used to locate a more precise curve at the top of the ridge provided by a new filtering stage with smaller σ_1 and σ_3 .

6. Evaluation of the procedure

In order to estimate the distortion introduced by our system 50 ECGs were acquired and digital recordings of 10 sec were stored on a digital support. For the validation ECG traces were obtained in different clinical conditions such as normal, supraventricular tachycardia, ventricular arrhythmias, previous myocardial infarction and left ventricular hypertrophy. The digital recordings were subsequently printed on traditional graph paper and processed with the procedure described above. Finally, the obtained signals were compared with the digital recordings by using a classical measure of ECG distortion such as the percentage root mean square difference (PRD) [3]. However, while the PRD is a global measure, every segment of the ECG signal has a different diagnostic meaning and significance. A distortion in an ECG segment does not necessarily have the same importance as a similar distortion in another segment. Therefore, the procedure was also evaluated with two mean opinion score (MOS) tests which were performed by three independent cardiologists [4]. A blind MOS error and a semi-blind MOS error were computed on the

ECG signals. The results of the tests (mean value \pm standard deviation) are illustrated in Table 1. As we can observe, the table shows a good correlation between the original and the reconstructed signals.

Index	Value
PRD	5.68 ± 1.87
Semi-blind MOS	4.25 ± 1.82
Blind MOS	5.13 ± 2.21

Table 1. The table (mean \pm standard deviation) shows a good correlation between the original and the reconstructed signals.

7. Conclusion

In this paper a method to convert ECG recordings on graph paper to digital signals is illustrated. The novelty of the paper is the utilization of the FOAM filter as a line edge detector. Although the procedure still need to be strengthened against wrinkles, scribbles and writings the experimental results show that the digital signal can be easily recovered and converted to a standard format.

References

- [1] M. Demi, M. Paterni, A. Benassi. The First Absolute Central Moment in Low-Level Image Processing. *Computer Vision and Image Understanding* 2000; vol.80 (1): 57-87.
- [1] Jian Tao Wang, Dinesh P. Mital. A microcomputer-based prototype for ECG paper record conversion. *Journal of Network and Computer Applications* 1996; vol.19: 295-307.
- [3] Yaniv Zigel, Arnon Cohen, Amos Katz. The Weighted Diagnostic Distortion (WDD) Measure for ECG Signal Compression. *IEEE Transactions on Biomedical Engineering* 2000; vol.47: 1422-1430.
- [4] Y. Zigel, A. Cohen, A. Abu-Ful, A. Wagshal, A. Katz. Analysis by Synthesis ECG Signal Compression. *Computers in Cardiology* 1997. IEEE Computer Society Press, 1997: 279-282.

Address for correspondence.

Marco Paterni
CNR Institute of Clinical Physiology
Via Moruzzi 1, 56100 Pisa, Italy

E-mail: paternim@ifc.cnr.it